JOURNAL OF Materials CHEMISTRY

Synthesis, characterisation and catalytic application of sol–gel processed cationic palladium(II) complexes†

Ekkehard Lindner,*[a] Andreas Baumann,[a] Peter Wegner,[a] Hermann A. Mayer,[a] Ulrich Reinöhl,[b] Achim Weber,[b] Teja S. Ertel[b] and Helmut Bertagnolli[b]

[a]Institut für Anorganische Chemie, Universität Tübingen, Auf der Morgenstelle 18, D-72076 Tübingen, Germany. E-mail: ekkehard.lindner@uni-tuebingen.de
[b]Institut für Physikalische Chemie, Universität Stuttgart, Pfaffenwaldring 55, D-70569 Stuttgart, Germany

Received 27th January 2000, Accepted 5th April 2000
Published on the Web 5th June 2000

The dicationic T-silyl functionalised bis(acetonitrile)(dppp)palladium(II) complex **2(T^0)** (see Scheme 1) was sol–gel processed with different amounts (y) of the co-condensation agent $MeSi(OMe)_2(CH_2)_6(MeO)_2SiMe$ **(D^0-C$_6$-D^0)** to give the new stationary phases **2a–h(T^n)(D^i-C$_6$-D^i)$_y$** ($y = 0$, 5, 10, 15, 20, 40, 80, and 100; $n = 0$–3, $i = 0$–2). The polysiloxane matrices and the integrity of the palladium(II) complex centres were investigated by means of solid state NMR (^{29}Si, ^{13}C, ^{31}P) and EXAFS spectroscopy. Dynamic NMR investigations show an increasing mobility of the hybrid polymers on going from $y = 0$ to 10. For higher amounts of the co-condensation agent $MeSiO_{i/2}(OX)_{2-i}(CH_2)_6O_{i/2}(XO)_{2-i}SiMe$ **(D^i-C$_6$-D^i)** the mobility tends toward that of a matrix consisting of **D^i-C$_6$-D^i** (T/D = 0) only. NMR experiments in suspension give further evidence for considerable mobility of the interphases (formed by the penetration of stationary and mobile phases on a molecular scale). Model reactions of **2a(T^n)** with different isocyanides in the interphase point to almost complete accessibility of the palladium(II) centres, even if the reactants carry sterically demanding substituents (*e.g. t*-Bu). The activity of the hybrid catalysts **2a–h(T^n)(D^i-C$_6$-D^i)$_y$** in the ethene/CO copolymerisation is markedly dependent on the temperature and the amount y of the co-condensation agent. A maximum of activity [1600 g(ECO) g(Pd)$^{-1}$ h^{-1}] is achieved with $y = 10$ which is 75% of the activity of the analogous homogeneous catalyst.

Introduction

The anchoring of transition metal complexes to an inert carrier matrix is regarded as an approach to combine the advantages of homogeneous and heterogeneous catalysis.[2–5] The sol–gel process offers a versatile and convenient route to generate stationary phases under mild conditions, consisting of a polysiloxane matrix, spacer and reactive centre.[6–10] In the presence of a mobile phase (gaseous, liquid or dissolved reactant) the gels (stationary phases) swell to form interphases in which (ideally) the reaction centres are in a solution-like state. An optimised cross linkage of the hybrid polymers and the binding of transition metals to polydentate ligands impedes their leaching within the interphase which is often a serious drawback of surface modified materials.[2,11–14]

The copolymerisation of T-silyl functionalised transition metal complexes with co-condensation agents like $MeSi(OMe)_2(CH_2)_6(MeO)_2SiMe$ **(D^0-C$_6$-D^0)** opens the opportunity to tailor the properties of interphase catalysts by varying the type and amount of the co-condensation agent.[1,15] However, mobility and cross linkage can not be tuned independently, since too many Si–O–Si bonds entail reduced flexibility.[1] To some extent this disadvantage is compensated by the application of specially designed co-condensation agents.[16,17] A further increase of mobility is achieved if the spacer is attached in the periphery of the ligand backbone.

Herein we wish to report on the synthesis and characterisation of dicationic palladium(II) complexes anchored to inorganic/organic hybrid polymers. The palladium(II) centre in these complexes is coordinated to a modified diphenylphosphinopropane ligand (dppp), in which the spacer is linked to the symmetric C_2 position of the alkyl chain.[18] The monomeric T-silyl functionalised complexes were sol–gel processed with different amounts of the co-condensation agent $MeSi(OMe)_2(CH_2)_6(MeO)_2SiMe$ **(D^0-C$_6$-D^0)**. The structural investigations of these novel stationary phases were carried out essentially by means of solid state NMR spectroscopy. This method gives information on structural dynamic properties of the new materials.[19–21] An exemplary examination of the environment of the palladium(II) centre was performed by EXAFS, since this method also operates in the case of amorphous materials.[22] Finally the polymeric palladium(II) complexes were applied as interphase catalysts in the copolymerisation of ethene with carbon monoxide[23] and their activity was investigated as a function of temperature and the amount of the co-condensation agent $MeSi(OMe)_2(CH_2)_6(MeO)_2SiMe$ **(D^0-C$_6$-D^0)**.

Results and discussion

Monomeric palladium(II) complex

The dicationic palladium(II) complex **2(T^0)** was obtained in quantitative yields as a highly viscous oil by replacing the chloro ligands in **1(T^0)** for acetonitrile in the presence of $AgSbF_6$ (Scheme 1).[24] The easy dissociation of both acetonitrile ligands is observed in the FD-MS spectrum of **2(T^0)**, in which the signal at $m/z = 723$ is assigned to the [$M^+ - 2$ MeCN] fragment. In the $^{31}P\{^1H\}$ NMR spectrum of **2(T^0)** a single ^{31}P peak is observed at δ 18.9.

Sol–gel processing of 2(T^0) with different amounts of the co-condensation agent D^0-C$_6$-D^0

In previous investigations it was demonstrated that $MeSi(OMe)_2(CH_2)_6(MeO)_2SiMe$ **(D^0-C$_6$-D^0)** is an excellent co-condensation agent, because it combines the remarkable mobility

---

†Supported Organometallic Complexes Part 19. Part 18: ref. 1.

DOI: 10.1039/b000744g

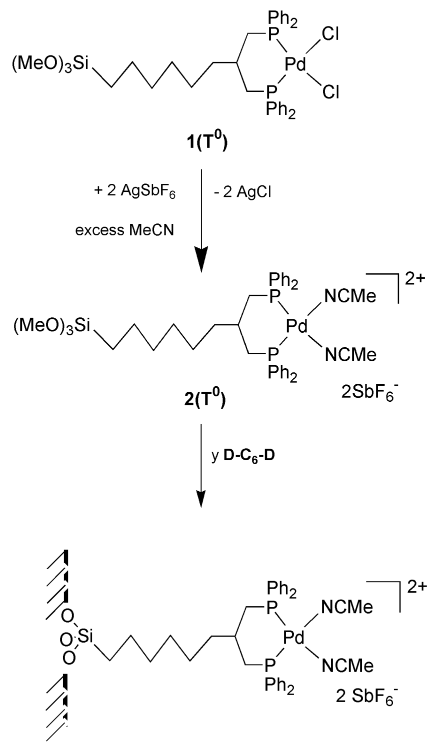

$\mathbf{2a(T^n)}$ $(y = 0)$
$\mathbf{2b(T^n)(D^i\text{-}C_6\text{-}D^i)_y}$ $(y = 5)$
$\mathbf{2c(T^n)(D^i\text{-}C_6\text{-}D^i)_y}$ $(y = 10)$
$\mathbf{2d(T^n)(D^i\text{-}C_6\text{-}D^i)_y}$ $(y = 15)$
$\mathbf{2e(T^n)(D^i\text{-}C_6\text{-}D^i)_y}$ $(y = 20)$
$\mathbf{2f(T^n)(D^i\text{-}C_6\text{-}D^i)_y}$ $(y = 40)$
$\mathbf{2g(T^n)(D^i\text{-}C_6\text{-}D^i)_y}$ $(y = 80)$
$\mathbf{2h(T^n)(D^i\text{-}C_6\text{-}D^i)_y}$ $(y = 100)$

T = T type silicon atom (three oxygen neighbours)
D = D type silicon atom (two oxygen neighbours)
n, i = Number of Si-O-Si bonds (n = 0 - 3, i = 0 - 2)
y = Amount of co-condensate

Scheme 1 Synthesis of the cationic palladium(II) complex $\mathbf{2(T^0)}$ and of the cationic hybrid palladium(II) complexes $\mathbf{2a\text{–}h(T^n)(D^i\text{-}C_6\text{-}D^i)_y}$ ($y = 0$–100).

of D groups with the cross linkage of Q functions, without the disadvantage of monofunctional D groups, which are easily washed out during the solvent processing after the sol–gel process.[16]

The adjustment of the density and distance of the reaction centres, which is an important tool to improve the activity of a catalyst, *via* the sol–gel process of $\mathbf{2(T^0)}$ succeeded with different amounts of the co-condensation agent $\mathbf{D^0\text{-}C_6\text{-}D^0}$ (the $\mathbf{D^0\text{-}C_6\text{-}D^0/T}$ ratio ranges between 0 and 100). In this way also the potential formation of less active metal clusters can be avoided. The properties of sol–gel processed materials strongly depend on the applied reaction conditions such as concentration of the starting materials, amount and type of solvent, temperature, reaction time, drying conditions of the wet gel, and type of catalyst. To ensure the same reaction kinetics for the synthesis of each polymer as a prerequisite for comparable results, the adherence to uniform reaction conditions has to be maintained during the entire hydrolysis and polycondensation procedure.[1,2,8,10] Methanol was added during the sol–gel process to homogenise the reaction mixture. $(n\text{-Bu})_2Sn(OAc)_2$ is an appropriate catalyst, which does not interfere with the reactive centre.[25] If these preconditions are carefully considered all stationary phases (Scheme 1) are reproducible and provided with the same respective properties.

Solid state NMR spectroscopic investigation of the hybrid catalysts

Several NMR active nuclei incorporated into the gels at specific sites allow the characterisation of different regions of the new materials. Whereas ^{31}P CP/MAS NMR spectroscopy affords direct access to the reactive centre, the ^{13}C nuclei provide information about the hydrocarbon backbone of the ligand and the alkyl spacer unit of the co-condensation agent. With ^{29}Si the polymeric matrix is investigated, in particular the degree of condensation, type and amount of D- and T-silyl species, and the realistic stoichiometry of the polymers.[2]

^{29}Si CP/MAS NMR spectroscopy

Typical chemical shifts of D groups are −2.2 (D^0), −13.6 (D^1), and −22.4 ppm (D^2). Because the two D-silyl groups of the $\mathbf{D^i\text{-}C_6\text{-}D^i}$ unit are held together *via* six methylene groups, D^0 species are not necessarily washed out like their monomer homologues in the course of the preparation of the stationary phase. T-silyl units give rise to resonances at −52.3 (T^1), −60.3 (T^2), and −68.3 ppm (T^3), respectively.

All silicon atoms in the polysiloxane matrix are in direct proximity of protons, thus all silyl species are detected *via* cross polarisation (Fig. 1).[12,13] The degree of condensation of D and T moieties and realistic T/D ratios were determined by contact time variation experiments (Table 1).[26,27] However, due to the low concentration of T-silyl functions in the stationary phases of $\mathbf{T:D^i\text{-}C_6\text{-}D^i}$ ratios $\leqslant 20$ the T groups can hardly be detected in the ^{29}Si CP/MAS NMR spectra. Therefore contact time experiments to determine the realistic stoichiometry of these materials are not feasible within a reasonable time.

The degree of condensation decreases with higher amounts of the co-condensation agent $\mathbf{D^0\text{-}C_6\text{-}D^0}$, resulting in jelly-like gels. In the course of the polycondensation the mobility of the $\mathbf{D^0\text{-}C_6\text{-}D^0}$ molecules is gradually reduced due to the formation of Si–O–Si bonds. If the sol–gel process quickly yields solid gels, as was found in the case of higher amounts of $\mathbf{D^0\text{-}C_6\text{-}D^0}$, the possibility to further form Si–O–Si bonds is deteriorated. In gels with a $\mathbf{D^0\text{-}C_6\text{-}D^0/T}$ ratio of 40 D^1-silyl groups are predominating. The relative intensity of the ^{29}Si signal of the fully cross-linked D^2 sub-unit drops to 30%. The stationary phase $\mathbf{2a(T^n)}$ without any co-condensation agent exhibits a rather high cross-linkage with a degree of condensation of 83% typically found for hybrid polymer systems being provided only with T functions.[15]

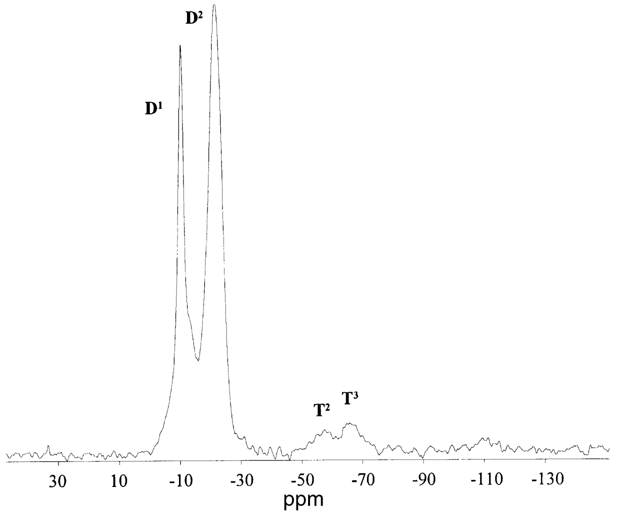

Fig. 1 ^{29}Si CP/MAS NMR spectrum of the copolymer $\mathbf{2b(T^n)(D^i\text{-}C_6\text{-}D^i)_5}$. Peaks due to the various silyl species are indicated.

Table 1 Relative I_0, T_{SiH} and $T_{1\rho H}$ data of the silyl species in the Fn-T/D-C$_6$-D copolymers

	Relative I_0 data of D and T species[a]					Degree of condensation [%]		Ratio complex/ cocondensation agent		T_{SiH}/ms[b]					
Compound	D^0	D^1	D^2	T^2	T^3	D	T	[b]	[c]	D^0	D^1	D^2	T^2	T^3	$T_{1\rho H}$/ms[b]
2a(T^n)				102.0	100		83.2	1/0					1.40	1.93	8.25
2b(T^n)(D^i-C$_6$-D^i)$_5$		61.7	100	4.9	6.7	80.9	85.9	1/7.0	1/6.7		1.24	1.3	0.7	1.1	10.8
2c(T^n)(D^i-C$_6$-D^i)$_{10}$		77.1	100	3.1	4.6	78.3	86.7	1/11.6	1/13.4		1.25	1.3	1.3	1.5	23.7
2d(T^n)(D^i-C$_6$-D^i)$_{15}$	10.4	11.9	100	1.2	2.6	83.0	89.2	1/16.8	1/12.5	3.14	1.59	1.29	0.9	1.91	12.4
2e(T^n)(D^i-C$_6$-D^i)$_{20}$	9.7	10.3	100	[d]	[d]	87.6			1/19.6	4.53	1.19	1.36	[e]	[e]	13.4
2f(T^n)(D^i-C$_6$-D^i)$_{40}$		140.5	100	[d]	[d]	70.8			1/47.1		1.23	1.30	[e]	[e]	8.3
2g(T^n)(D^i-C$_6$-D^i)$_{80}$		250.9	100	[d]	[d]	64.3			1/93.8		1.30	1.33	[e]	[e]	7.0
2h(T^n)(D^i-C$_6$-D^i)$_{100}$		164.9	100	[d]	[d]	68.9			1/110		1.15	1.23	[e]	[e]	

[a] I_0 values calculated according to literature methods. [b] Determined by contact time variation. [c] Determined *via* deconvolution of ^{29}Si CP/MAS NMR spectra. [d] Species not detectable. [e] Intensity too low for a precise determination.

^{13}C CP/MAS NMR spectroscopy

The ^{13}C CP/MAS spectra of the hybrid polymers **2a–h(T^n)(D^i-C$_6$-D^i)$_y$** reveal signals in the aromatic regions originating from the phenyl carbon atoms of the dppp ligand. The resonances of the different methylene carbon atoms in the aliphatic section of **2a(T^n)** cannot be resolved. In the case of **2b–h(T^n)(D^i-C$_6$-D^i)$_y$** however, three major signals (δ 33.3, 23.2, and 17.9) are dominating this region, which are assigned to the methylene groups of the spacer unit. The resonances of these carbon atoms shift to lower field with increasing distance to the silicon. The small signal at δ 49.6 for the Si–OMe functions indicates a high degree of hydrolysis. The signal at δ 13.8 is ascribed to the carbon atom adjacent to the silicon atom of the T moiety. The methyl group of the co-condensation agent gives rise to a signal at δ −0.3.

^{31}P CP/MAS NMR and IR spectroscopic investigations

The hybrid polymers **2a–h(T^n)(D^i-C$_6$-D^i)$_y$** give rise to one single ^{31}P peak at δ 19 flanked by spinning side bands. This chemical shift correlates well with that of the monomeric precursor complex **2(T^0)**. No decomposition products were found after the sol–gel process.

To protect both vacant coordination sites in the hybrid polymers **2a–h(T^n)(D^i-C$_6$-D^i)$_y$**, which are necessary for the copolymerisation of ethene with carbon monoxide, easily replaceable acetonitrile was employed. The presence of this coordinating solvent in the materials was evidenced IR spectroscopically. An absorption at 2237 cm^{-1} is characteristic for the C≡N stretching vibration.

EXAFS spectroscopic characterisation of 2a(T^n)

Due to the amorphous nature of the stationary phases, no information about the structure of the reactive palladium centre is available by means of X-ray diffraction. EXAFS, however, allows the determination of the first coordination sphere of the palladium atom, since this method is independent of the nature of the material.[22] The k^3-weighted EXAFS function of **2a(T^n)** (Fig. 2) is described best by three different shells. The first peak in the corresponding Fourier transform is mainly due to the phosphorus atoms of the diphos ligand, but the nitrogen atoms of the acetonitrile ligands also contribute significantly. Because of the small difference of their distances to the absorber, these backscatterers cause only one single peak in the Fourier transform. A less intense peak at about 3.3 Å is assigned to the carbon atoms of the acetonitrile ligands. Contrary to the expectation the inclusion of multiple scattering effects for the Pd–N–C unit did not improve the fit. This can be explained by the strong scattering from the diphos group which dominates the spectra to such an extent that multiple scattering effects from the Pd–N–C groups become relatively insignificant. Alternatively a change in the binding properties leading to a deviation from linearity of the Pd–N–C angle cannot be excluded. This is the case in the complex [(bis(dipropylphosphino)propane)Pd(NCMe)$_2$][BF$_4$]$_2$ the structure of which was determined by an X-ray structural analysis.[28] However, since the Pd–C distance (see below) indicates an angle of ~180°, the latter assumption is less probable. The coordination numbers of the backscatterers were fixed at the expected values in order to reduce the number of independent parameters.

Some important interatomic distances, in particular those between palladium and the ligand, are summarised in Table 2. The obtained lengths are in good agreement with those determined for the above mentioned similar palladium complex.[28] Whereas the Pd–P distances are nearly equal (2.24 *vs.* 2.25 Å), the Pd–N bonds differ slightly (2.17 *vs.* 2.11 Å). Assuming a C–N bond length of 1.16 Å, which is the known value for acetonitrile, the Pd–C distance of 3.3 Å corresponds well with the sum of the Pd–N and C–N bond lengths (2.15 Å + 1.16 Å ≈ 3.31 Å).

Dynamic studies by solid state NMR spectroscopy

To develop new hybrid catalysts for chemistry in interphases it is not only essential to know structural aspects of stationary phases, equally important is their dynamic behaviour. Enhanced mobility results in higher accessibility and uniformity of the reactive centres and thus in improved activities and selectivities in catalysis.[2,15] NMR parameters like relaxation and cross polarisation constants are sensitive toward motion, giving access to dynamic properties of the materials in different time scales.[27,29]

Dynamic behaviour of the stationary phases

If the cross-polarisation constant T_{XH} and the relaxation time of the protons in the spin-lock field $T_{1\rho H}$ are detected *via* ^{29}Si CP/MAS NMR spectroscopy direct information is accessible about the mobility of the different D- and T-silyl species within the polysiloxane network. Differences in the $T_{1\rho H}$ values are

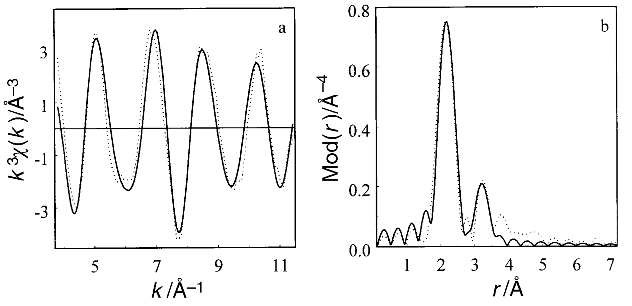

Fig. 2 Calculated (solid line) and experimental (dotted line) $k^3\chi(k)$ function (a) and their Fourier transforms (b) (Pd K-edge) in the k-range of 3.7–11.5 Å^{-1}.

Table 2 EXAFS spectroscopically determined structural data absorber backscatterer distance r [Å], coordination number N and Debye–Waller factor σ [Å] of $\mathbf{2a(T'')_2}$, energy shift $\Delta E_0 = 26.2 \pm 0.5$ eV

	r/Å	N	σ/Å
Pd–N	2.15 (±0.03)	2	0.084 (±0.02)
Pd–P	2.24 (±0.02)	2	0.067 (±0.01)
Pd–C	3.33 (±0.03)	2	0.045 (±0.02)

attributed to improved or impaired mobility in the kHz region, since these changes affect the dipolar coupling among protons.[30,31] Moreover, $T_{1\rho H}$ is an averaged quantity for all protons within a given volume of up to 1–2 nm in diameter, whenever an efficient spin diffusion process is present. Temperature dependent investigations of the $T_{1\rho H}$ relaxation times of the hybrid materials **2b(T″)(D^i-C$_6$-D^i)$_5$**, **2c(T″)(D^i-C$_6$-D^i)$_{10}$**, **2f(T″)(D^i-C$_6$-D^i)$_{40}$**, and **2g(T″)(D^i-C$_6$-D^i)$_{80}$** result in increasing $T_{1\rho H}$ values on going from 298 to 335 K. This indicates that the $T_{1\rho H}$ values of the investigated materials are on the left side of the correlation time curve. In this fast motion regime large $T_{1\rho H}$ values correspond to high mobility.[19] Upon decreasing the ratio between **2a(T″)** and the co-condensation agent to 1 : 10 the mobility increases (Table 1, Fig. 3). If this ratio is in the range between 1 : 15 and 1 : 40 a decrease of the relaxation rate $T_{1\rho H}$ is observed indicating a reduced mobility of the stationary phases. Thus the incorporation of **D^i-C$_6$-D^i** groups into the highly cross-linked T-networks of **2a(T″)** breaks up the rigid matrix which in the first place results in an enhancement of the dynamics. By further adding **D^i-C$_6$-D^i** groups the material is dominated by the network of the stationary phase of **(D^i-C$_6$-D^i)$_y$** which is less mobile than a mixture of **2a(T″)** and **D^i-C$_6$-D^i** in a 1 : 10 ratio. Therefore the mobility decreases until the dynamic behaviour of pure **(D^i-C$_6$-D^i)$_y$** is reached (Table 1, Fig. 3). This agrees well with the decay of the cross polarisation constants T_{SiH} of the D^1 and D^2 groups of the hybrid catalysts **2b–h(T″)(D^i-C$_6$-D^i)$_y$**, which approach those T_{SiH} relaxation rates found for matrices containing exclusively the material **D^i-C$_6$-D^i**.[16] For the cross polarisation constants T_{SiH} of the D^1 groups a limiting value of 1 ms is detected, while for those of the D^2-silyl species an approximate value of 1.3 ms is achieved.

The $T_{1\rho H}$ values of all materials investigated display a monoexponential decay which is in favour of a homogeneous distribution of the functionalised palladium(II) complexes in the stationary phases.

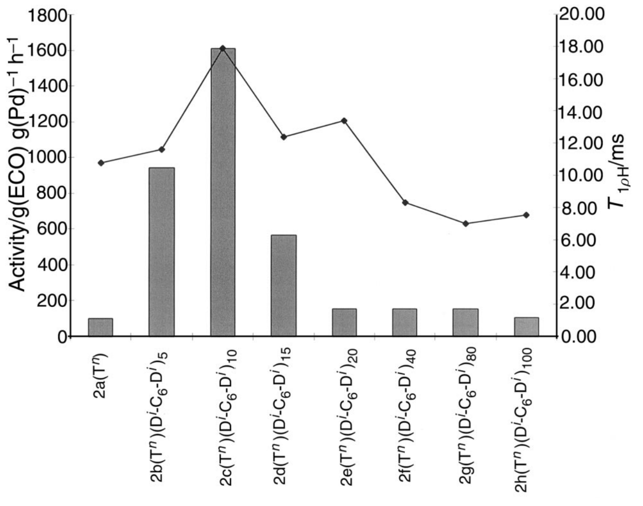

Fig. 3 Activity of the hybrid catalysts **2a(T″)** and **2b(T″)(D^i-C$_6$-D^i)$_5$**–**2h(T″)(D^i-C$_6$-D^i)$_{100}$** (bars) *versus* the relaxation rate of the protons in the rotating frame $T_{1\rho H}$ (measured *via* ^{29}Si line).

NMR investigations in the interphase

Since reactions take place in swollen gels, interphases were also studied by means of NMR spectroscopy in suspension. As examples the hybrid materials **2a(T″)** and **2c(T″)(D^i-C$_6$-D^i)$_{10}$** were swollen in different solvents (mobile phases) and transferred into a MAS rotor. To prevent phase separation the samples were spun not faster than 3500 Hz during the NMR experiments. ^{1}H NMR spectroscopy revealed proton spectra of good quality which allowed the assignment of the different proton sites (Fig. 4). This effect points to a high mobility which prevents cross polarization.[29] The proton suspension NMR spectra of **2a(T″)** reveal a dependence on the applied solvent, with CD_2Cl_2 achieving the best resolution. Even in the case of the signal originating from aromatic protons different sites can be distinguished as shoulders within the broad resonance. ^{1}H signals at δ 3.5 and 3.7 are ascribed to the aliphatic protons of the dppp ligand backbone, while both high field resonances at δ 2.4 and 0.7 are assigned to the protons of the spacer unit. The chemical shifts are compatible with those of the monomeric precursors **2(T^0)**. Although the ^{1}H NMR spectra displayed a good resolution the quality of the ^{13}C{^{1}H} NMR spectrum of **2a(T″)** under low power solution state conditions suffers from long repetition delays and relaxation rates T_1 of the carbon atoms as well as of short relaxation rates T_2 and thus the lack of an adequate signal to noise ratio.

Model reactions in the interphase

One of the most important factors for the successful performance of a reaction in interphases is the accessibility of the reactive centres for incoming substrates. An indispensable precondition for that is only ensured if diffusion problems are restrained. Highly mobile stationary phases and solution-like interphases offer a valuable possibility to overcome such problems. As an example the polymeric complex **2a(T″)** swollen in dichloromethane was treated under ambient conditions with isonitriles of different steric demand like *n*-butyl, cyclohexyl, and *tert*-butyl isocyanide (Scheme 2). The IR spectra of the products **3a(T″)**, **3b(T″)**, and **3c(T″)** show two strong NC absorptions at lower wave numbers as compared to the non-coordinated isonitriles. In the ^{31}P CP/MAS NMR spectra of **3a–c(T″)** one signal is detected for the equivalent phosphorus atoms at a chemical shift of δ 7. No resonances of the starting material **2a(T″)** are found indicating a sufficient accessibility of the reactive centres in the interphase.

Ethene/CO copolymerisation

Transition metal catalysts anchored to polymeric carriers play an increasing role, because the products can be easily separated from the catalytically active centres. Moreover in the cases of

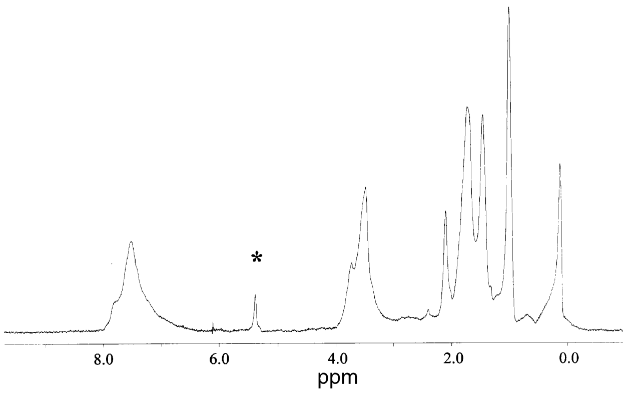

Fig. 4 ^{1}H NMR spectrum (in suspension) of **2d(T″)(D^i-C$_6$-D^i)$_{15}$** swollen in CD_2Cl_2. (* residual non-deuterated solvent peak).

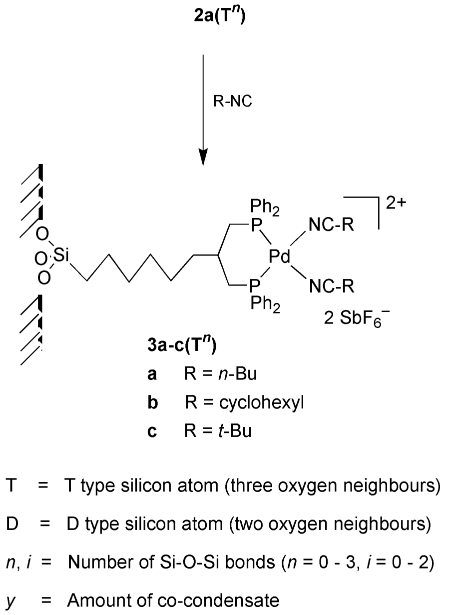

Scheme 2 Model reactions of the cationic hybrid palladium(II) complex $\mathbf{2a(T^n)}$ with isocyanides.

supported metallocenes the solvent-free production of polypropylene is highly profitable. Also the morphology of the polymer can be controlled.[32] Since metallocenes are of homogeneous nature their application in gas phase or slurry reactors causes "reactor fouling". This drawback is avoided if metallocenes are immobilised on inert carrier matrices like silica or zeolites.[33]

Similar problems can arise in the copolymerisation of ethene with carbon monoxide leading to polyketones. To avoid reactor fouling in this type of copolymerisation different hybrid catalysts $\mathbf{2b–h(T^n)(D^i\text{-}C_6\text{-}D^i)_y}$ (Scheme 1) were used. In particular the influence of an increasing amount of the co-condensation agent $\mathbf{D^0\text{-}C_6\text{-}D^0}$ on the activity of the catalyst was tested. Each of the stationary phases was swollen in a CH_2Cl_2/MeOH mixture of 20 : 1 and a reaction time of 16 h was selected. The catalytic runs were carried out at two different temperatures (24 and 50 °C) and the results were compared with those of the homogeneous palladium catalyst $[(dppp)Pd(CNMe)_2][SbF_6]_2$. As expected the activities of the catalysts increased dramatically if the temperature was raised from 24 to 50 °C (Fig. 5). A considerable enhancement of the activity (factor of 15) is observed on going from $\mathbf{2a(T^n)}$ to $\mathbf{2c(T^n)(D^i\text{-}C_6\text{-}D^i)_{10}}$. At 50 °C the efficiency of this hybrid catalyst is about 75% of that of the dicationic complex $[(dppp)Pd(CNMe)_2][SbF_6]_2$ in homogenous phase under the same conditions (1600 *vs.* 2100 g(ECO) $g(Pd)^{-1}\ h^{-1}$).[28] With higher amounts of the co-condensation agent ($y > 10$), however, the activity declines and achieves a value of only 100 g(ECO) $g(Pd)^{-1}\ h^{-1}$ with $y = 100$ (Fig. 3). The appearance of a maximum in the activity can not only be traced back to the corresponding maximum of mobility of the carrier matrix, but also to an optimum of the density of the reaction centres. A higher dilution of the palladium complexes within the matrix causes the diffusion to become the rate determining step, which explains the catalytic behaviour of the palladium complexes with $y > 10$. Increasing the amount of the co-condensation agent leads to ethene/carbon monoxide copolymers of a higher molecular mass. However, the molecular weight distribution ranges between 7 and 10 (Table 3). The polyketone is soluble in hexafluoroisopropanol. Hence the insoluble catalyst can be separated by filtration. In the solution no palladium was detected by atomic absorption spectroscopy indicating that no metal leaching took place.

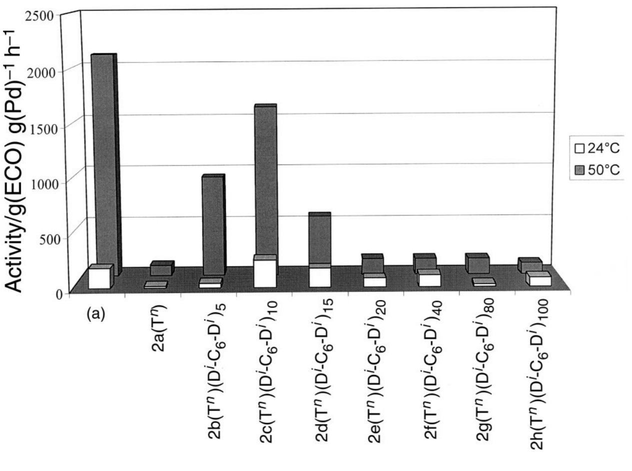

Fig. 5 Activity of the inorganic/organic hybrid catalysts $\mathbf{2a(T^n)}$ and $\mathbf{2b(T^n)(D^i\text{-}C_6\text{-}D^i)_5–2h(T^n)(D^i\text{-}C_6\text{-}D^i)_{100}}$ in dependence on the amount of the co-condensation agent $\mathbf{D^i\text{-}C_6\text{-}D^i}$ in a mixture of CH_2Cl_2/MeOH. ((a) Activity of the analogous homogenous complex under these conditions).

Conclusion

The application of sol–gel processed T-silyl functionalised dicationic (dppp)palladium(II) complexes for alternating ethene/carbon monoxide copolymerisation in interphases represents another example of the successful combination of the advantages of homogeneous and heterogeneous catalysis.[2,15] A further benefit of interphase catalysts is the avoidance of reactor fouling. The activity of the hybrid catalysts depends on the mobility of the reactive centre which can be influenced by the type and amount of the employed co-condensation agent. To increase the stability of the matrix, a large number of Si–O–Si bonds is necessary. However, such a high cross linkage exerts a negative impact on the mobility. Since high mobility is an important factor for the catalytic activity a compromise has to be reached between cross linkage and mobility. A suitable co-condensation agent is $MeSi(OMe)_2(CH_2)_6(MeO)_2SiMe$ ($\mathbf{D^0\text{-}C_6\text{-}D^0}$) which meets the mentioned requirements.

Yet, according to solid state NMR investigations (^{31}P, ^{29}Si, ^{13}C), the dynamic behaviour of the stationary phase consisting of the matrix, the spacer unit, and the reactive centre can not be increased indefinitely. With increasing amounts of the co-condensation agent $\mathbf{D^0\text{-}C_6\text{-}D^0}$ ($y > 40$) the flexibility of the polymer tends toward that of the undiluted sol–gel processed polysiloxane $\mathbf{D^i\text{-}C_6\text{-}D^i}$. The observed catalytic activities, however, do not completely reflect the above-mentioned findings, since with increasing amounts of the co-condensation agent the density and the distance of the reactive centres have also to be taken into account. A higher dilution implicates a lower concentration of the catalytically active centres and the diffusion becomes the rate determining step. For a y value of 10 (50 °C) the hybrid catalyst $\mathbf{2c(T^n)(D^i\text{-}C_6\text{-}D^i)_y}$ exhibits the

Table 3 Molecular weights of the ethene/carbon monoxide copolymers as a function of the co-condensation agent

Compound	Molecular weight		Polydispersity
	M_w/g mol^{-1}	M_n/g mol^{-1}	M_w/M_n
$\mathbf{2a(T^n)}$	223000	22000	10.1
$\mathbf{2b(T^n)(D^i\text{-}C_6\text{-}D^i)_5}$	494000	55000	9.0
$\mathbf{2c(T^n)(D^i\text{-}C_6\text{-}D^i)_{10}}$	500000	61000	8.2
$\mathbf{2d(T^n)(D^i\text{-}C_6\text{-}D^i)_{15}}$	[a]	[a]	[a]
$\mathbf{2e(T^n)(D^i\text{-}C_6\text{-}D^i)_{20}}$	640000	91000	7.0
$\mathbf{2f(T^n)(D^i\text{-}C_6\text{-}D^i)_{40}}$	720000	105000	6.9
$\mathbf{2g(T^n)(D^i\text{-}C_6\text{-}D^i)_{80}}$	[a]	[a]	[a]
$\mathbf{2h(T^n)(D^i\text{-}C_6\text{-}D^i)_{100}}$	[a]	[a]	[a]

[a] Not determined.

highest activity in the ethene/carbon monoxide copolymerisation, reaching up to 75% of the analogous homogeneous (dppp)palladium(II) complex under comparable reaction conditions.

For a successful performance of an interphase catalyst the accessibility of the reactive centres is of considerable relevance. Model reactions of **2a(T″)** with isocyanides bolstered a nearly complete accessibility of the palladium(II) centres.

Experimental

Physical measurements

Elemental analyses were carried out on a Carlo Erba Model 1106 analyzer and on a Vario EL (Fa. Elementar Analytische Systeme, Hanau); Cl analyses were performed according to Dirschel and Erne[34] and Schöniger.[35] Solution state nuclear magnetic resonance spectra (NMR) were recorded on a Bruker DRX 250 spectrometer at 298 K. Frequencies were as follows: $^{31}\mathrm{P}\{^{1}\mathrm{H}\}$ NMR: 101.25 MHz, referenced to 85% H_3PO_4; $^{13}\mathrm{C}\{^{1}\mathrm{H}\}$ NMR: 62.90 MHz; all $^{13}\mathrm{C}\{^{1}\mathrm{H}\}$ NMR spectra were referenced relative to partially deuterated solvent peaks which are reported relative to tetramethylsilane (TMS). Mass spectra (field desorption) were acquired on a Finnigan MAT 711A instrument (8 kV, 333 K) modified by AMD (Harpsted, Germany) and are reported as mass/charge (*m*/*z*). IR data were obtained on a Bruker IFS 48 FT-IR spectrometer.

CP/MAS solid-state NMR spectra were recorded on Bruker MSL and DSX 200 (4.7 T) multinuclear spectrometers (^{29}Si) and on a Bruker ASX 300 (7.05 T) spectrometer (^{13}C and ^{31}P) equipped with wide bore magnets. Magic angle spinning was applied at 3.5 kHz (^{29}Si) and 10–12 kHz (^{13}C, ^{31}P). All samples were packed under exclusion of molecular oxygen. Frequencies and standards: ^{31}P, 121.49 MHz (85% H_3PO_4, $NH_4H_2PO_4$ as secondary standard); ^{13}C, 50.325 MHz [TMS, carbonyl resonance of glycine ($\delta = 170.09$) as secondary standard]; ^{29}Si, 39.75 MHz (Q_8M_8). The cross polarization constants T_{PH} and T_{SiH} were determined by variations of the contact time (20–25 experiments). The proton relaxation time in the rotating frame $T_{1\rho\mathrm{H}}$ was measured by direct proton spinlock–τ–CP experiments.[30] $T_{1\mathrm{P}}$ values were determined using the method developed by Torchia.[36] The relaxation time data were obtained using the Bruker software SIMFIT or Jandel software PEAKFIT. Peak deconvolution of the spectra was performed with the Bruker-Spectrospin software XWINNMR using Voigtian line shapes. For the quantification of the silyl species in all polysiloxanes, ^{29}Si CP/MAS NMR contact time variations experiments were carried out.

The suspension NMR measurements were performed on a Bruker ASX 300 spectrometer, as used for the solid state NMR experiments (*vide infra*), without the high power amplifier using the standard multinuclear solid state probe head at room temperature (20 °C). Frequency: ^{1}H NMR: 300.13 MHz. For the ^{1}H suspension measurements, the heteronuclear channel was tuned to ^{2}H for locking purposes and the samples were swollen in deuterated solvents, which were degassed prior to use. The samples were rotated at the magic angle at 3500 Hz.

The EXAFS measurement of **2a(T″)** was performed at the palladium K-edge (24350 eV) at the beamline A1 of the Hamburger Synchrotronstrahlungslabor (HASYLAB) at DESY, Hamburg under ambient conditions, positron energy 4.5 GeV and initial beam current 120 mA. For harmonic rejection, the second crystal of the Si(311) double crystal monochromator was tilted to 30%. Data were collected in transmission mode with ion chambers flushed with argon. The energy was calibrated with a palladium foil of 5 μm thickness. The sample itself was prepared by pressing a mixture of 240 mg of **2a(T″)** and 40 mg of polyethylene to a tablet of 1.3 cm diameter and 0.2 cm thickness.

EXAFS data were analyzed with a program package developed for the investigation of amorphous solids.[37] Background subtraction was done with AUTOBK from the University of Washington, the evaluation in *k*-space was performed with the EXCURV92 module xalpha potentials and phaseshifts of the program package CERIUS2.[38,39] The mean free path of the scattered electrons was calculated from the imaginary part of the potential (VPI was set to −4.0), the amplitude reduction factor AFAC was fixed at 0.8, and an overall energy shift E_0 was introduced to obtain the best fit to the experimental data. The coordination numbers of the backscatteres were fixed at the known values in order to reduce the number of independent parameters.

Preparations

All manipulations were performed under an atmosphere of argon by employing usual Schlenk techniques. All solvents were dried according to common methods, and were distilled and stored under argon. THF was freshly distilled from sodium/benzophenone prior to use. The catalytic reactions were carried out in autoclaves with volumes of 100 and 150 ml. The reactions were controlled by a specially designed computer program.[40] To monitor the temporal progress of the pressure and temperature, all autoclaves were equipped with computer controlled sensors, which recorded both pressure and temperature each minute, yielding information on the progress of the copolymerization. The palladium complex **1(T^0)** and the co-condensation agent **D^0-C$_6$-D^0** were synthesized according to literature methods. $(n\text{-Bu})_2Sn(OAc)_2$ was purchased from Merck (Darmstadt, Germany), distilled and stored under argon. Ethene and carbon monoxide were a gift from BASF Aktiengesellschaft.

Bis(acetonitrile)(2-diphenylphosphinomethyl-1-diphenylphosphino-8-trimethoxysilyloctane)palladium(II)bis(hexafluoroantimonate) [2(T^0)]. To a solution of **1(T^0)** (620 mg, 0.795 mmol) in THF (5 ml) and acetonitrile (5 ml) was added a solution of $AgSbF_6$ (546 mg, 1.59 mmol) in THF (10 ml). The reaction mixture was stirred for 1 h under exclusion of light and precipitated AgCl was removed by centrifugation. Then the solvent was removed under reduced pressure and **2(T^0)** was obtained as a highly viscous orange oil in quantitative yields. $^{13}\mathrm{C}\{^{1}\mathrm{H}\}$ NMR (CD_3CN): δ 134.6–127.5 (m, C-phenyl), 48.6 ($SiOCH_3$), 32.8 (CH_2P), 30.0 ($CH(CH_2)_3$), 28.0–21.0 (CH_2), 11.4 ($SiCH_2$); $^{31}\mathrm{P}\{^{1}\mathrm{H}\}$ NMR (CD_3CN): δ 19.2; IR (THF): 2324, 2293 cm^{-1} (C≡N); MS (FD): *m*/*z* (%): 727 ($M^+ - 2$ MeCN). Anal. calc. for $C_{40}H_{52}F_{12}N_2O_3P_2PdSb_2Si$ (1276.81): C, 38.72; H, 4.06; N, 2.19. Found: C, 39.35; H, 4.44; N 1.56%.

Sol–gel processing. To a solution of **2(T^0)** in 5 ml of THF/acetonitrile (1 : 1) the corresponding amount of the co-condensation agent **D^0-C$_6$-D^0** was added. For the homogenization of this mixture methanol (30 μg) and as a catalyst $(n\text{-Bu})_2Sn(OAc)_2$ (30 mg) were employed and the reaction mixture was stirred at room temperature in a sealed Schlenk tube for 12 h until a gel was formed. Then the solvent was removed under reduced pressure and the obtained gels were dried for 2 h *in vacuo*. After washing three times with toluene (30 ml, 4 h), diethyl ether (30 ml, 4 h) and *n*-pentane (30 ml, 4 h) and drying for 8 h *in vacuo* the gels were obtained as yellow to brown powders.

Bis(acetonitrile)(2-diphenylphosphinomethyl-1-diphenylphosphino-8-polysiloxanyloctane)palladium(II)bis(hexafluoroantimonate) 2a(T″). Initial weight of **2(T^0)** 215 mg, 0.169 mmol; ^{31}P CP/MAS NMR: δ 18.0; ^{13}C CP/MAS NMR: δ 146.0–114.6 (C-phenyl), 42.6–15.4 (CH_2, CH), 11.5 (CH_2Si), 0.8 (CH_3CN); ^{29}Si CP/MAS NMR: δ −55.6 (**T^2**, $I_0 = 1.24$), −65.0 (**T^3**, $I_0 = 1.22$);

IR (KBr): 2324, 2297 cm^{-1} (C≡N). Anal. calc. for $C_{37}H_{43}F_{12}N_2O_{3/2}P_2PdSb_2Si$ (idealised stoichiometry): C, 36.80; H, 3.59; N, 2.26. Corrected stoichiometry:[41] C, 36.80; H, 3.60; N, 2.3. Found: C, 33.33; H, 3.16; N, 1.56%.

2b(T^n)(D^i-C$_6$-D^i)$_5$. Initial weights of **D^0-C$_6$-D^0** 530 mg, 1.80 mmol and of **2(T^0)** 460 mg, 0.36 mmol; ^{31}P CP/MAS NMR: δ 19.9; ^{13}C CP/MAS NMR: δ 146.0–117.4 (C-phenyl), 53.3 (SiOCH$_3$), 33.3 ($\mathit{C}H_2CH_2CH_2Si$), 27.0 (CH$_2$, CH), 23.19 ($CH_2\mathit{C}H_2CH_2Si$), 17.9 ($CH_2CH_2\mathit{C}H_2Si$), 13.8 (CH$_2$Si), -0.2 (SiCH$_3$); ^{29}Si CP/MAS NMR: δ 12.4 (**D^1**, $I_0=0.95$), -22.4 (**D^2**, $I_0=1.3$), 58.5 (**T^2**, $I_0=0.08$), -67.8 (**T^3**, $I_0=0.1$); IR (KBr): 2324 cm^{-1} (C≡N). Anal. calc. for $C_{77}H_{133}F_{12}N_2O_{21.5}P_2PdSb_2Si_{11}$ (idealised stoichiometry): C, 45.49; H, 6.59; N, 1.38. Corrected stoichiometry:[41] C, 44.15; H, 7.10; N, 0.78. Found: C, 41.95; H, 6.66; N, 0.62%.

2c(T^n)(D^i-C$_6$-D^i)$_{10}$. Initial weights of **D^0-C$_6$-D^0** 500 mg, 1,69 mmol and of **2(T^0)** 215 mg, 0.169 mmol; ^{31}P CP/MAS NMR: δ 19.9; ^{13}C CP/MAS NMR: δ 146.0–117.4 (C-phenyl), 53.3 (SiOCH$_3$), 33.3 ($\mathit{C}H_2CH_2CH_2Si$), 27.0 (CH$_2$, CH), 23.19 ($CH_2\mathit{C}H_2CH_2Si$), 17.9 ($CH_2CH_2\mathit{C}H_2Si$), 13.8 (CH$_2$Si), -0.2 (SiCH$_3$); ^{29}Si CP/MAS NMR: δ -9.6 (**D^1**, $I_0=1.0$), -21.7 (**D^2**, $I_0=1.3$), -59.4 (**T^2**, $I_0=0.02$), -67.0 (**T^3**, $I_0=0.03$); IR (KBr): 2326 cm^{-1} (C≡N). Anal. calc. for $C_{117}H_{22}F_{12}N_2O_{21.5}P_2PdSb_2Si_{21}$ (idealised stoichiometry): C, 47.39; H, 7.58; N, 0.94. Corrected stoichiometry:[41] C, 44.15; H, 7.10; N, 0.78. Found: C, 38.69; H, 6.11; N, 0.94%.

2d(T^n)(D^i-C$_6$-D^i)$_{15}$. Initial weights of **D^0-C$_6$-D^0** 500 mg, 1.69 mmol and of **2(T^0)** 215 mg, 0,169 mmol; ^{31}P CP/MAS NMR: δ 19.9; ^{13}C CP/MAS NMR: δ 146.0–117.4 (C-phenyl), 53.3 (SiOCH$_3$), 33.3 ($\mathit{C}H_2CH_2CH_2Si$), 27.0 (CH$_2$, CH), 23.19 ($CH_2\mathit{C}H_2CH_2Si$), 17.9 ($CH_2CH_2\mathit{C}H_2Si$), 13.8 (CH$_2$Si), -0.2 (SiCH$_3$); ^{29}Si CP/MAS NMR: δ -2.5 (**D^0**, $I_0=0.13$), -12.4 (**D^1**, $I_0=0.16$), -22.4 (**D^2**, $I_0=1.3$), -58.5 (**T^2**, $I_0=0.02$), -67.8 (**T^3**, $I_0=0.03$); IR (KBr): 2330 cm^{-1} (C≡N). Anal. calc. for $C_{117}H_{22}F_{12}N_2O_{21.5}P_2PdSb_2Si_{31}$ (idealised stoichiometry): C, 43.48; H, 6.95; N, 0.87. Corrected stoichiometry:[41] C, 44.59; H, 7.54; N, 0.61. Found: C, 44.10; H, 6.94; N, 1.06%.

2e(T^n)(D^i-C$_6$-D^i)$_{20}$. Initial weights of **D^0-C$_6$-D^0** 500 mg, 1.69 mmol and of **2(T^0)** 107 mg, 0.085 mmol; ^{31}P CP/MAS NMR: δ 19.0; ^{13}C CP/MAS NMR: δ 141.5–115.6 (C-phenyl), 49.8 (SiOCH$_3$), 33.4 ($\mathit{C}H_2CH_2CH_2Si$), 27.0 (CH$_2$, CH), 23.3 ($CH_2\mathit{C}H_2CH_2Si$), 17.9 ($CH_2CH_2\mathit{C}H_2Si$), 13.9 (CH$_2$Si), -0.1 (SiCH$_3$), -5.4 (SiCH$_3$ of D^0 groups); ^{29}Si CP/MAS NMR: δ -2.3 (**D^0**, $I_0=0.13$), -13.1 (**D^1**, $I_0=0.13$), -22.5 (**D^2**, $I_0=1.3$); IR (KBr): 2330 cm^{-1} (C≡N); Anal. calc. for $C_{197}H_{403}F_{12}N_2O_{41.5}P_2Pd\ Sb_2Si_{41}$ (idealised stoichiometry): C, 45.02; H, 7.73; N, 0.53. Corrected stoichiometry:[41] C, 44.98; H, 7.71; N, 0.54. Found: C, 44.51; H, 7.72; N, 1.38%.

2f(T^n)(D^i-C$_6$-D^i)$_{40}$. Initial weights of **D^0-C$_6$-D^0**: 500 mg, 1.69 mmol and of **2(T^0)**: 53.5 mg, 0.042 mmol; ^{31}P CP/MAS NMR: δ 19.1; ^{13}C CP/MAS NMR 138.8–119.6 (C-phenyl), 49.8 (SiOCH$_3$), 33.5 ($\mathit{C}H_2CH_2CH_2Si$), 23.2 ($CH_2\mathit{C}H_2CH_2Si$), 17.7 ($CH_2CH_2\mathit{C}H_2Si$), -0.1 (SiCH$_3$); ^{29}Si CP/MAS NMR: δ -9.7 (**D^1**, $I_0=1.28$), -12.3 (**D^1**, $I_0=0.72$), -21.9 (**D^2**, $I_0=1.4$), -56.7 (**T^2**); IR (KBr): 2324 cm^{-1} (C≡N). Anal. calc. for $C_{357}H_{763}F_{12}N_2O_{81.5}P_2PdSb_2Si_{81}$ (idealised stoichiometry): C, 46.09; H, 8.27; N, 0.30. Corrected stoichiometry:[41] C, 46.27; H, 8.36; N, 0.26. Found: C, 45.51; H, 8.08; N, 0.08%.

2g(T^n)(D^i-C$_6$-D^i)$_{80}$. Initial weights of **D^0-C$_6$-D^0** 500 mg, 1.69 mmol and of **2(T^0)** 25 mg, 0.02 mmol; ^{31}P CP/MAS NMR: δ 20.0; ^{13}C CP/MAS NMR: δ 138.8–118.3 (C-phenyl), 33.4 ($\mathit{C}H_2CH_2CH_2Si$), 23.2 ($CH_2\mathit{C}H_2CH_2Si$), 17.6 ($CH_2CH_2\mathit{C}H_2Si$), -0.2 (SiCH$_3$); ^{29}Si CP/MAS NMR: δ -9.7 (**D^1**, $I_0=3.18$), -20.8 (**D^2**, $I_0=1.3$); IR (KBr): 2326 cm^{-1} (C≡N). Anal. calc. for $C_{677}H_{1483}F_{12}N_2O_{161.5}P_2PdSb_2Si_{161}$ (idealised stoichiometry): C, 46.73; H, 8.59; N, 0.16; Corrected stoichiometry:[41] C, 46.85; H, 8.64; N, 0.14. Found: C, 44.33; H, 6.72; N, 0.083%.

2h(T^n)(D^i-C$_6$-D^i)$_{100}$. Initial weights of **D^0-C$_6$-D^0** 500 mg, 1.69 mmol and of **2(T^0)** 21.5 mg, 0.017 mmol; ^{31}P CP/MAS NMR: δ 20.9; ^{13}C CP/MAS NMR: δ 135.7–124.0 (C-phenyl), 33.4 ($\mathit{C}H_2CH_2CH_2Si$), 23.1 ($CH_2\mathit{C}H_2CH_2Si$), 17.6 ($CH_2CH_2\mathit{C}H_2Si$), -0.2 (SiCH$_3$); ^{29}Si CP/MAS NMR: δ -9.7 (**D^1**, $I_0=3.2$), -21.4 (**D^2**, $I_0=2.8$), -56.6 (**T^2**, $I_0=0.04$), -66.7 (**T^3**, $I_0=0.02$); IR (KBr): 2331 cm^{-1} (C≡N). Anal. calc. for $C_{837}H_{1843}F_{12}N_2O_{201.5}P_2PdSb_2Si_{201}$ (idealised stoichiometry): C, 46.87; H, 8.66; N, 0.13. Corrected stoichiometry:[41] C, 46.93; H, 8.69; N, 0.12. Found: C, 44.32; H, 8.42; N, 0.014%.

Model reactions

The stationary phase **2a(T^n)** (200 mg, 0.166 mmol) was transferred into the interphase by mixing **2a(T^n)** with CH$_2$Cl$_2$ (5 ml). Then the respective isocyanide (0.5 ml) was added and the reaction mixture was stirred for 4 h. The solvent and excess reactant were removed under reduced pressure and the stationary phases **3a–c(T^n)** were obtained.

Bis(*n*-butylisocyanide)(2-diphenylphosphinomethyl-1-diphenylphosphino-8-polysiloxanyloctane)palladium(II)bis(hexafluoroantimonate) [3a(T^n)]. ^{31}P CP/MAS NMR: δ 6.9; ^{13}C CP/MAS NMR: δ 135.7–124.0 (C-phenyl), 41.8–18.8 (CH$_2$, CH); IR (KBr): 2255, 2203 cm^{-1} (C≡N). Anal. calc. for $C_{43}H_{55}F_{12}N_2O_{1.5}P_2PdSb_2Si$ (idealised stoichiometry): C, 41.99; H, 4.51; N, 2.28. Corrected stoichiometry:[41] C, 42.00; H, 4.50; N, 2.29. Found: C, 39.95; H, 4.30; N, 2.94%.

Bis(cyclohexylisocyanide)(2-diphenylphosphinomethyl-1-diphenylphosphino-8-polysiloxanyloctane)palladium(II)bis(hexafluoroantimonate) [3b(T^n)]. ^{31}P CP/MAS NMR: δ 7.5; ^{13}C CP/MAS NMR: δ 163.2 (CN), 135.7–124.0 (C-phenyl), 62.0 (*C*-CN), 32.8 (CH$_2$, cyclohexyl), 31.0–18.8 (CH$_2$, CH); IR (KBr): 2255, 2203 cm^{-1} (C≡N). Anal. calc. for $C_{43}H_{55}F_{12}N_2O_{1.5}P_2PdSb_2Si$ (idealised stoichiometry): C, 41.99; H, 4.51; N, 2.28. Corrected stoichiometry:[41] C, 42.00; H, 4.50; N, 2.29. Found: C, 45.00; H, 2.39; N, 2.87%.

Bis(*tert*-butylisocyanide)(2-diphenylphosphinomethyl-1-diphenylphosphino-8-polysiloxanyloctane)palladium(II)bis(hexafluoroantimonate) [3c(T^n)]. ^{31}P CP/MAS NMR: δ 6.8; ^{13}C CP/MAS NMR: δ 135.7–124.0 (C-phenyl), 41.8–18.8 (CH$_2$, CH); ^{29}Si CP/MAS NMR: δ -56.6 (**T^2**, $I_0=0.04$), -66.7 (**T^3**, $I_0=0.02$); IR (KBr): 2185, 2244 cm^{-1} (C≡N). Anal. calc. for $C_{43}H_{55}F_{12}N_2O_{1.5}P_2PdSb_2Si$ (idealised stoichiometry): C, 41.99; H, 4.51; N, 2.28. Corrected stoichiometry:[41] C, 42.00; H, 4.50; N, 2.29. Found: C, 39.61; H, 4.22; N, 3.93%.

Preparation of the ethene/carbon monoxide copolymers

In a typical run a 100 or 150 ml autoclave was charged with 15 mg of the respective complex **2a−h(T^n)(D^i-C$_6$-D^i)$_y$**, which was swollen in 21 ml of a mixture of dichloromethane and methanol (20 : 1). The autoclave was pressurized with 30 bar of ethene and carbon monoxide each, then heated to the reaction temperature and the contents of the autoclaves were vigorously stirred. After the reaction was completed, the autoclave was cooled to room temperature and the remaining gases were vented. Finally the solvent was removed and the polyketone was obtained as a colorless powder, being insoluble in all common organic solvents with the exception of a mixture of hexafluoroisopropanol and toluene. No reactor fouling was observed. Mp 255 °C (decomp.); ^{13}C{^{1}H} NMR (CF$_3$CH(OH)CF$_3$/[D$_8$]toluene, 25 °C): δ 211.6 (C=O), 35.1

(CH_2); ^{13}C CP/MAS NMR: δ 210.0 (C=O), 35.6 (CH_2); IR (KBr): 1691 cm^{-1} (C=O). Anal. calc. for $(C_3H_4O)_n$ (56.03): C, 64.27; H, 7.19. Found: C, 63.74; H, 6.87%.

Acknowledgements

The support of this research by the Deutsche Forschungsgemeinschaft (Forschergruppe, Grant No. Li 154/41-4), Bonn Bad Godesberg, and by the Fonds der Chemischen Industrie, Frankfurt/Main, is gratefully acknowledged. We are grateful to Degussa AG for a generous gift of $PdCl_2$ and the BASF Aktiengesellschaft for the donation of carbon monoxide and ethene. Furthermore we wish to thank HASYLAB at DESY, Hamburg, for the provision of synchrotron radiation and technical support. We are grateful to BASF Aktiengesellschaft for the provision of ethene and carbon monoxide as well as the GPC measurements.

References

1 E. Lindner, W. Wielandt, A. Baumann, H. A. Mayer, U. Reinöhl, A. Weber, T. S. Ertel and H. Bertagnolli, *Chem. Mater.*, 1999, **11**, 1833.
2 E. Lindner, F. Auer, T. Schneller and H. A. Mayer, *Angew. Chem.*, 1999, **111**, 2155; E. Lindner, F. Auer, T. Schneller and H. A. Mayer, *Angew. Chem., Int. Ed. Engl.*, 1999, **38**, 2154.
3 F. R. Hartley, *Supported Metal Complexes*, D. Reidel Publishing Company, Dordrecht, 1985.
4 U. Schubert, *New J. Chem.*, 1994, **18**, 1049.
5 W. A. Herrmann and B. Cornils, *Angew. Chem.*, 1997, **109**, 1074; W. A. Herrmann and B. Cornils, *Angew. Chem., Int. Ed. Engl.*, 1997, **36**, 2057.
6 C. J. Brinker and G. W. Scherer, *Sol–Gel Science*, Academic Press, London, 1990.
7 E. Lindner, M. Kemmler, H. A. Mayer and P. Wegner, *J. Am. Chem. Soc.*, 1994, **116**, 348.
8 D. A. Loy and K. J. Shea, *Chem. Rev.*, 1995, **95**, 1431 and references cited therein.
9 R. Corriu and D. Leclercq, *Angew. Chem.*, 1996, **108**, 1524; R. Corriu and D. Leclercq, *Angew. Chem., Int. Ed. Engl.*, 1996, **35**, 1420.
10 L. L. Hench and J. K. West, *Chem. Rev.*, 1990, **90**, 33.
11 U. Deschler, P. Kleinschmit and P. Panster, *Angew. Chem.*, 1986, **98**, 237; U. Deschler, P. Kleinschmit and P. Panster, *Angew. Chem., Int. Ed. Engl.*, 1986, **25**, 237.
12 D. W. Sindorf and G. E. Maciel, *J. Am. Chem. Soc.*, 1983, **105**, 3767.
13 E. Bayer, K. Albert, J. Reiners, M. Nieder and D. Müller, *J. Chromatogr.*, 1983, **264**, 197.
14 J. Blümel, *Inorg. Chem.*, 1994, **33**, 5050.
15 E. Lindner, T. Schneller, F. Auer, P. Wegner and H. A. Mayer, *Chem. Eur. J.*, 1997, **3**, 1833.
16 E. Lindner, T. Schneller, H. A. Mayer, H. Bertagnolli, T. S. Ertel and W. Hoerner, *Chem. Mater.*, 1997, **9**, 1524.
17 E. Lindner, T. Salesch, F. Höhn and H. A. Mayer, *Z. Anorg. Allg. Chem.*, 1999, **625**, 2133.
18 E. Lindner, A. Enderle and A. Baumann, *J. Organomet. Chem.*, 1998, **558**, 235.
19 C. A Fyfe, *Solid State NMR for Chemists*, CRC Press, Guelph, 1984.
20 G. Engelhardt and D. Michel, *High Resolution NMR of Silicates and Zeolites*, John Wiley and Sons, Chichester, New York, Brisbane, Toronto, Singapore, 1987.
21 H. Eckert, *Prog. Nucl. Magn. Reson. Spectrosc.*, 1992, **24**, 159.
22 H. Bertagnolli and T. S. Ertel, *Angew. Chem.*, 1994, **106**, 15; H. Bertagnolli and T. S. Ertel, *Angew. Chem., Int. Ed. Engl.*, 1994, **33**, 45.
23 E. Drent and P. H. M. Budzelaar, *Chem. Rev.*, 1996, **96**, 663.
24 (*a*) A. Sen and T.-W. Lai, *J. Am. Chem. Soc.*, 1982, **104**, 3520; (*b*) A. Sen and T.-W. Lai, *Organometallics*, 1984, **3**, 866.
25 E. Lindner, R. Schreiber, T. Schneller, P. Wegner, H. A. Mayer, W. Göpel and C. Ziegler, *Inorg. Chem.*, 1996, **35**, 514.
26 The degree of condensation of the T species: 100 $(T^1+2T^2+3T^3)/[3(T^1+T^2+T^3)]$, degree of condensation of the D species: 100 $(D^1+2D^2)/[(2D^0+D^1+D^2)]$; T^1, T^2, T^3, D^0, D^1, D^2 are the relative amounts of silyl species present in the sample (Table 1).
27 R. K. Harris, *Analyst*, 1985, **110**, 649.
28 E. Lindner, M. Schmid, J. Wald, J. A. Queisser, M. Geprägs, P. Wegner and C. Nachtigal, *J. Organomet. Chem.*, in press.
29 K. Schmidt-Rohr and H. W. Spiess, *Multidimensional Solid State NMR and Polymers*, Academic Press, London, 1994.
30 J. Schaefer, E. O. Steijskal and R. Buchdahl, *Macromolecules*, 1977, **10**, 384.
31 A. D. Torchia, *J. Magn. Reson.*, 1978, **30**, 613.
32 B. Steinmetz, J. Zechlin, C. Przybyla, B. Tesche and G. Fink, *Nachr. Chem.*, 2000, **48**, 12.
33 H. G. Alt, *J. Chem. Soc., Dalton Trans.*, 1999, 1703.
34 A. Dirschel and F. Erne, *Microchim. Acta*, 1961, 866.
35 (*a*) W. Schöniger, *Microchim. Acta*, 1955, 123; (*b*) W. Schöniger, *Microchim. Acta*, 1956, 869.
36 A. D. Torchia, *J. Magn. Reson.*, 1978, **30**, 613.
37 T. S. Ertel, H. Bertagnolli, S. Hueckmann, U. Kolb and D. Peter, *Appl. Spectrosc.*, 1992, **46**, 690.
38 M. Newville, P. Livins, Y. Yakobi, J. J. Rehr and E. A. Stern, *Phys. Rev. B*, 1993, **47**, 14126.
39 S. J. Gurman, N. Binsted and I. Ross, *J. Phys. C*, 1986, **19**, 1845.
40 P. Wegner, computer program for the control of high pressure autoclaves, University of Tübingen, 1999.
41 The corrected stoichiometry was obtained by adding the additional number of OH units of the D^0, D^1, D^2, T^1, T^2, and T^3 groups (obtained from the ^{29}Si CP/MAS NMR spectra) of the idealised stoichiometry (only D^2 and T^3 units). The real T/D ratio and the degree of hydrolysis were also taken into account.